cigre Turkey

TEPES
TURKISH JOURNAL OF ELECTRICAL POWER AND ENERGY SYSTEMS

TEPES, Vol. 4, Issue. 2, 108-117, 2024 **DOI:** 10.5152/tepes.2024.24007

REVIEW

A Comprehensive Review of Physics-Based Battery Models and Comparing Different Physics-Based Models for Various Chemistries

Hakki Yavuz[1], Arda Akyildiz[1,2], Mehmet Onur Gulbahce[1,2]

[1]Department of Electrical Engineering, İstanbul Technical University, İstanbul, Türkiye
[2]ITU Advanced Vehicle Technologies Application and Research Center, ILATAM İstanbul, Türkiye

Cite this article as: H. Yavuz, A. Akyildiz and M. O. Gulbahce, "A comprehensive review of physics-based battery models and comparing different physics-based models for various chemistries," *Turk J Electr Power Energy Syst.*, 2024; 4(2), 108-117.

ABSTRACT

The increasing importance of batteries across diverse sectors, spanning from consumer electronics to electric vehicles, underscores the critical necessity for precise battery models. This review delineates four primary categories of battery models: empirical, equivalent circuit, data-driven, and physics-based models. Empirical models like the Nernst and Shepherd models offer simplicity but lack precision. Equivalent circuit models strike a balance between simplicity and accuracy, albeit with validation constraints. Data-driven methods leverage machine learning to predict battery performance accurately but require high-quality datasets. Physics-based models integrate fundamental electrochemical processes for detailed understanding, albeit with heightened computational complexity. Comparative analyses, with a focus on lithium-ion batteries, reveal trade-offs between computational efficiency and accuracy. The Single Particle Model and its extension single particle model with electrolyte dynamics emerge as efficient options, with single particle model with electrolyte dynamics showing promising accuracy akin to Single Particle Model. Additionally, comparisons across different battery chemistries unveil varying levels of modeling precision. This article compares different electrochemical modeling techniques across chemistries to discern optimal methods. The electrochemical model, which is one of the battery modeling techniques, has been examined and investigated in detail in this study and has contributed to the literature on how the model with which chemistry works with which electrochemical model. In addition, this study contributed to the existing lithium ferro-phosphate chemistry modeling with optimization technique in pybamm. The synthesis offers insights into diverse modeling methodologies and their implications for battery research and development, guiding future investigations toward more tailored modeling strategies for specific applications.

Index Terms—Lithium-ion battery, electrochemical modeling, comparing modeling methods

I. Introduction

In today's world, the importance of batteries, which are energy storage systems used in almost all electronic devices in our lives, ranging from electric vehicles to consumer electronics, medical devices, industrial applications, aerospace, and defense, is increasing every day. Batteries are devices that store and provide electrical energy through reversible chemical reactions. While batteries with various chemistries are used today, the most popular type of battery is lithium-ion batteries. Lithium-ion batteries are widely used in electric vehicles, consumer electronics, and energy storage systems since they have high energy density, low self-discharge, and are lightweight. They are available in various chemistries such as Lithium Cobalt Oxide (LiCoO2), Lithium Iron Phosphate (LiFePO4), and Lithium Nickel Manganese Cobalt Oxide (NMC). The increasing significance of these batteries is directly dependent on the effective harnessing of their capabilities. Achieving this level of efficiency and utility necessitates the development of precise and actionable battery models.

In literature, battery models are categorized into four main groups [1]. The classical empirical models, based on experiments, include the Shepherd model [2], the Unnewehr universal model [3, 4], and the Nernst model [5]. The Nernst model is noted for its accuracy, while the Shepherd model is particularly effective for continuous discharge currents. Enhancements to these models involve adding more parameters and variables. For example, improving the Nernst model's prediction of dynamic terminal voltage is possible by incorporating two constants (τ1 and τ2) [6]. Additionally, refining the Nernst model with the hysteresis effect offers further improvements [7]. However, such enhancements increase computational complexity. The accuracy of these three models in predicting terminal voltage is compared in [8].

Received: April 7, 2024
Revision Requested: May 2, 2024
Last Revision Received: May 6, 2024
Accepted: May 13, 2024
Publication Date: June 20, 2024

Corresponding author: Mehmet Onur Gulbahce, ogulbahce@itu.edu.tr

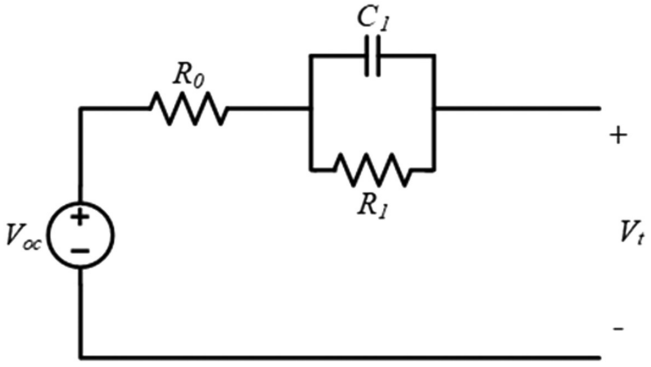

Fig. 1. Equivalent circuit model (ECM).

Secondly, the equivalent circuit model (ECM) consists of a SOC-dependent voltage source, an internal resistor, and resistance-ca pacitance (RC) networks that can describe the electrical relationship between the inputs (current, SOC, and temperature) and the terminal voltage [9]. Fig. 1 illustrates a schematic of a part of a simple electrical circuit that contains resistors (R_0 and R_1) and a capacitor (C). The model comprising an internal resistor and a resistor-capacitor block between the open circuit voltage and the terminal voltage is used as a common battery model [10]. When contrasting ECMs with empirical models, it becomes evident that ECMs exhibit a high degree of simplification in their ability to accurately discern the electrical properties inherent to batteries. Besides, because of the large number of circuit components and their variations, the ECM gives researchers enough flexibility to design a structure appropriate for their application. By adding more elements, the model can yield more correct and precise simulations of battery behavior. The disadvantage of using more elements in the equivalent circuit is that more information about the cell is needed for parameterization and CPU time for calculations increases [11]. The empirical battery model can give accurate outputs, but the model requires validation for all different scenarios. ECMs are used for various industrial applications due to their simple structure and simple parameterization process. But the model can only be applied to the scenarios for which it has been tested and processes such as aging are difficult to incorporate, so adaptation and new data collection are required [12].

Data-driven battery modeling methods aim to predict battery performance and capacity using information derived from large datasets.

Main Points

- Summarized and compared various modeling methods in existing literature based on their complexity and outcomes.
- Explored the relationship between these modeling methods and specific chemistries, aiming to discern which methods are more suitable for particular chemical systems.
- Updated modeling approaches with optimization methods to enhance accuracy, and investigated which chemistries are better suited for physics-based modeling understanding.

Their increasing popularity stems from their ability to model complex nonlinear behaviors, adaptability, and high accuracy rates. These models employ machine learning techniques to understand the relationship between input parameters like voltage, temperature, current, and output parameters such as state of charge and capacity, based on a dataset of battery measurements. However, the use of these models requires a careful experimental setup and data collection process, as high-quality data is essential. The use of unstable data can lead to the model overfitting or underpredicting [13, 14].

Physics-based models, also known as electrochemical models, mathematically express the fundamental physical and chemical processes in batteries, including electrochemical reactions, ion transport, electron flow, and the materials' thermodynamic and kinetic properties. Lithium-Ion flow among the solid and electrolyte phases is oftentimes involved in these models, along with charge and mass conservation in both phases. The electrochemical model is represented in the form of nonlinear Partial Differential Equations (PDEs). For this reason, a precondition for utilizing an electrochemical model to derive a direct analytical solution is to turn the PDEs into Ordinary Differential Equations (ODEs). Numerical techniques such as integral approximation, Pade approximation, Ritz method, finite element method, and finite difference method are often preferred to discretize nonlinear PDEs in electrochemical models [15, 16]. Employing these models enables accurate predictions of battery performance under various conditions, including charge-discharge cycles, temperature variations, and aging effects.

There are many electrochemical models in the literature; these offer various approaches to understanding the complex internal structure and operational mechanisms of batteries. Electrochemical battery modeling comprehensively addresses the electrochemical reactions of the battery, thermal management, electrical characteristics, and aging processes. These models provide insights into how batteries will perform under real-world conditions, assisting in the development of design and operational strategies necessary to make batteries more efficient and longer-lasting.

In [17], it was first used to determine the parameters that extract the model of the LFP cell, presents simulations of power and capacity degradation of LiFePO4-Graphite Li-ion batteries by simplifying the electrochemical and thermal aging model. They developed a model to understand how the performance of LFP cells changes with time. The model simulates the degradation in the capacity and power of the battery, taking into account thermal as well as electrochemical interactions. This study can be considered as an important step towards understanding the aging processes of LiFePO4-Graphite Li-ion batteries and improving their performance. Since other modeling attempts using the parameters presented in [17] did not yield the desired modeling results, an additional study [18] was conducted in 2021 to optimize the parameters and find variations and parameters that produce more accurate results.

In [19, 20], a method for determining the electrochemical model of a lithium-ion battery, with a focus on lithium polymer battery cell, is introduced. A series of experiments and analyses are performed to develop a comprehensive model that includes electrochemical

and thermal properties as well as material properties. First, several chemical experiments were conducted to determine the electrochemical properties of the lithium-ion battery. These experiments were carried out to identify the material properties of the electrodes, the diffusion rates of lithium ions, and the electrochemical reaction kinetics. Then, physical experiments were made to determine the material properties and thermal behavior. These experiments were carried out to evaluate the conductivity properties of the electrode materials, temperature profiles, and thermal conductivities of the lithium-ion battery. The data obtained were used to determine the parameters of the electrochemical model used to simulate the behavior of the battery. This study provides a contribution to more accurate modeling of lithium-ion batteries and a better understanding of their performance. In addition to this model, some of the parameters used in the study, which will be discussed later, are tab placement parameters taken from measurements in [21] and some electrode and electrolyte properties from [22].

In [22], an electrochemical, thermal, and mechanical model that investigates the nonuniform distribution of stress within lithium-ion pouch cells, with a focus on lithium cobalt oxide-graphite cell, is described. The model adopts a pseudo-2D approach involving mechanically coupled diffusion physics, which enables the study of the stress response in electrode particles. The results obtained in the study indicate that the model can successfully predict voltage, temperature, and thickness variations in pouch cells and are in agreement with experimental data.

To implement all these modeling techniques and to ensure the safety and longer useful life of the lithium-ion battery for its better operation, there is an important and fundamental need for a battery management system (BMS). The battery management system should have the capability to provide accurate prediction to the state of charge (SOC), state of battery integrity, and remaining useful life in the cell. Estimating the state of charge of the battery is one of the most important features of BMS tasks. Yet, the SOC is difficult to predict accurately. This is because SOC is the internal state of the battery cell and is not directly measured. Therefore, the SOC must be estimated. So far, several methods have been proposed to estimate the state of charge of the battery, which are generally divided into two groups: free model and model-based. Free models include Ampere-hour (Ah) or coulomb count, open circuit voltage (OCV). Apart from these two methods, the development reported in [23-25] is the method that applies a particle filter modified with the RLS algorithm to improve the accuracy of predicting the SOC of a lithium-ion battery in electric vehicles. The results show that the proposed method works effectively compared to other methods.

The following are the details for the 3 main categories most commonly found in the literature, but another similar approach is the Two-parameter approximation model, Single Particle Model (SPM), and Decoupled Solution Approach, which are also grouped into 3 main categories. Aging studies related to this classification were also performed for Lithium Manganese Oxide (LMO) cell and it was concluded that for the same electrolyte and cell parameters, the simulation methods can be applied to any cell chemistry [26].

II. ELECTROCHEMICAL BATTERY MODEL

Electrochemical battery models play a key role in understanding energy storage and conversion processes. These models typically incorporate a mix of electrochemical interactions, transport events, and circuit elements to truly describe the complex behavior of batteries. The electrochemical model of the mechanism can not only define macroscopic physical quantities such as voltage and current but also simulate important microscopic physical quantities inside the cell, which is suitable for application in degradation analysis and aging analysis of battery behavior [27-29].

Physics-based models provide a more detailed understanding by directly incorporating the electrochemical reactions and transport phenomena underlying the battery. These models are usually based on partial differential equations (PDEs) to describe the species concentration, charge, and temperature distributions within the battery. While more complex and computationally intensive compared to lumped-parameter models, physics-based models offer higher accuracy and can capture nuances such as temperature effects, electrolyte transport limitations, and electrode degradation. Hybrid approaches are also available, combining aspects of both granular parameter and physics-based models, aiming to strike a balance between computational efficiency and accuracy. Ultimately, the selection of the model depends on the specific application requirements, the level of detail needed, and the computational resources available.

A. Single Particle Model

The single particle model (SPM) is a representation of a Li-ion battery [Fig 2] that takes into account the transport of lithium ions within the solid particles of the battery electrodes. The model assumes a constant concentration of lithium ions in the electrolyte and ignores the propagation of the electrode concentration along the electrode. Diffusion within each electrode is ruled by Fick's law in the spherical orientation. Boundary conditions at the surface and core of the particle are defined to represent the intercalation-deintercalation process of lithium ions. The molar flux at the surface is influenced by the input current density and the diffusion rate constant. The Butler–Volmer equation considers the electrode concentration to be equal to the electrolyte concentration and associates the overpotential at the solid–electrolyte interface with the current density. Negative and positive phase overpotentials are expressed as functions of temperature, charge transfer coefficient, and electrode surface area. The exchange current density is calculated based on the constant electrolyte concentration and the maximum concentration of the electrode. The state of charge (SoC) of the battery can be determined using normalized lithium concentrations on the surface of the electrodes. The total cell potential takes into account contributions from the overpotentials of the electrodes and open circuit potential functions [19, 20]. SPM representation of Lithium-Ion batteries are illutrated in Fig. 2.

More detailed explanation of SPM and its formulas, SPM comprises of two diffusion equations that exhibit spherical symmetry: one operating within a typical negative particle ($k = n$) and the other within a typical positive particle ($k = p$). At the core of each particle, the standard no-flux condition is enforced. Given the SPM's assumption that

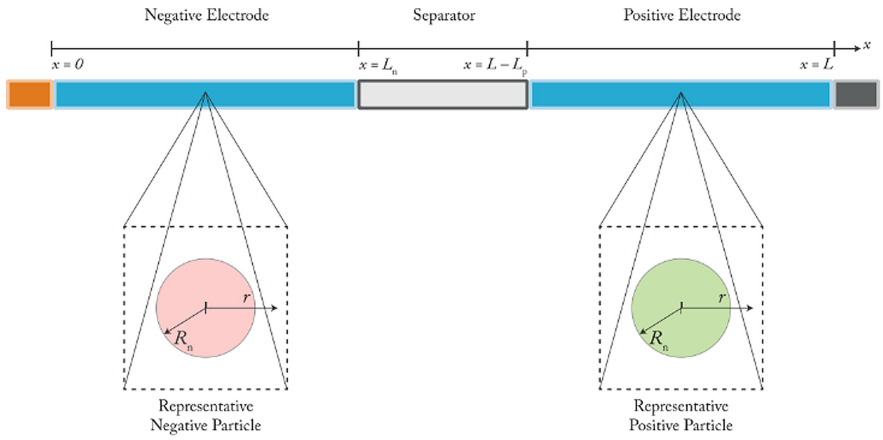

Fig. 2. SPM representation of lithium-ion batteries [23]. SPM, single particle model.

all particles within an electrode exhibit identical behavior, the flux at the particle surface equates to the current (I) divided by the electrode thickness (L_k). The concentration of lithium within electrode (k) is represented as (c_k). The model equations governing the SPM are as follows [24, 30]:

$$\frac{\partial_{c_{s,k}}}{\partial_t} = -\frac{1}{r_k^2}\frac{\partial}{\partial_{r_k}}\left(r_k^2 \mathrm{N}_{s,k}\right) \tag{1}$$

$$\mathrm{N}_{s,k} = -\mathrm{D}_{s,k}\left(c_{s,k}\right)\frac{\partial_{c_{s,k}}}{\partial_{r_k}}, \quad k \in n,p \tag{2}$$

$$\mathrm{N}_{s,k}\,|_{r_k=0} = 0,\ k \in n,p, \quad \mathrm{N}_{s,k}\,|_{r_k=1} = \begin{cases} \dfrac{1}{F_{a_n} L_n}, & k = n \\ -\dfrac{1}{F_{a_p} L_p}, & k = p \end{cases} \tag{3}$$

$$c_{s,k}\left(r_k, 0\right) = c_{s,k,0}, \quad k \in n,p \tag{4}$$

where $\mathrm{D}_{s,k}$ is the diffusion coefficient in the solid, $\mathrm{N}_{s,k}$ denotes the flux of lithium ions in the solid particle within the region k, and r_k is the radial coordinate of the particle in electrode k.

The voltage is obtained from the expression:

$$\begin{aligned} V = {} & U_p\left(c_p\right)|_{r_p=1} - U_n\left(c_n\right)|_{r_n=1} \\ & -\frac{2RT}{F}\sinh^{-1}\left(\frac{I}{2j_{0,p}a_p L_p}\right) \\ & -\frac{2RT}{F}\sinh^{-1}\left(\frac{I}{2j_{0,n}a_n L_n}\right) \end{aligned} \tag{5}$$

with the exchange current densities given by

$$\mathrm{j}_{0,k} = \left(c_k\right)^{1/2}\left(1 - c_k\right)^{1/2} \tag{6}$$

B. Single Particle Model with Electrolyte

Single particle model with electrolyte dynamics (SPMe) extends the single particle model (SPM) to cover electrolyte diffusion dynamics across the length of battery electrodes. It presents diffusion equations for the negative electrolyte, separator, and positive electrolyte, taking into account electrolyte polarization and conductivity due to overpotential.

The diffusion equations rule the electrolyte diffusion through the thickness of the electrodes and separator, with additional terms that represent the electrolyte polarization and conductivity. Boundary conditions provide stability of concentration at the interfaces between the different regions.

The electrolyte potential is divided into electrolyte overpotentials that rely on conductivity and electrolyte polarization. Electrolyte conductivity depends on concentration and is derived from experimental data. The effective conductivity is defined as a function of the lithium concentration and the volume fractions of each region, taking into account the porous structure of the electrolyte medium.

The Bruggeman correction is used to determine the effective conductivity and the Bruggeman exponent measures the influence of the porous medium on the electrolyte properties. Higher Bruggeman constants lead to lower effective conductivity, directly affecting the cell voltage.

The electrical overpotential due to electrolyte conductivity is represented as ohmic resistance, taking into account the current density and the thicknesses of the electrodes and separator. This resistance is identified by electrochemical impedance spectroscopy.

The electric overpotential due to lithium-ion diffusion is calculated based on the electrolyte activity coefficient, which takes into account the effects of electrolyte concentration and temperature. The activity coefficient is calculated separately for each phase.

Finally, the cell potential is calculated as the sum of the solid-phase potential (from SPM) and the electric overpotentials due to electrolyte conductivity and polarization.

Overall, SPMe provides a more comprehensive understanding of battery behavior by integrating electrolyte dynamics and its effect on cell performance and voltage.

More detailed explanation of SPMe and its formulas, SPMe encompasses equations governing the lithium concentration within representative particles situated in the negative electrode ($c_{s,n}$) and the positive electrode ($c_{s,p}$), alongside an equation dictating the behavior of the first-order correction to the lithium concentration within the electrolyte ($c_{e,k}$), where a Roman subscript $k \in n,s,p$ designates the negative electrode, separator, and positive electrode regions, respectively.

Adhering to the standard practice, the no-flux condition is enforced at the center of each particle, and the flux at the particle's surface is determined as the ratio of the current (I) to the thickness of the respective electrode (L_k), akin to the SPM. Given the transfer of lithium between the electrolyte and particles, the flux through the particle's surface is incorporated into the electrolyte diffusion equation as a source/sink term. Notably, there's no lithium transfer between the electrolyte and current collectors, resulting in no-flux boundary conditions on the lithium concentration within the electrolyte ($c_{e,k}$) at either end of the cell.

It is imperative to set initial conditions reflecting the establishment of an initial concentration within each particle ($c_{s,k}(t=0)=c_{s,k,0}$), and ensuring no deviation from the initial (uniform) lithium concentration within the electrolyte ($c_{e,k}\,(t=0)=c_{e,0}$) [24, 30]:

Particle formulas are given in (7)–(9) where $\mathrm{D_{s,k}}$ is the diffusion coefficient in the solid, $\mathrm{N_{s,k}}$ denotes the flux of lithium ions in the solid particle within the region k, and r_k is the radial coordinate of the particle in electrode k.

$$\frac{\partial_{c_{s,k}}}{\partial_{\mathrm{t}}} = -\frac{1}{r_k^2}\frac{\partial}{\partial_{r_k}}\left(r_k^2 \mathrm{N_{s,k}}\right) \tag{7}$$

$$\mathrm{N_{s,k}} = -\mathrm{D_{s,k}}\left(c_{s,k}\right)\frac{\partial_{c_{s,k}}}{\partial_{r_k}}, \quad k \in n,p, \tag{8}$$

$$\mathrm{N_{s,k}}\,|_{r_k=0} = 0 \; k \in n,p, \quad \mathrm{N_{s,k}}\,|_{r_k=1} = \begin{cases} \dfrac{1}{F_{a_n} L_n}, & k=n, \\ -\dfrac{1}{F_{a_p} L_p}, & k=p, \end{cases} \tag{9}$$

Electrolyte formulas are given in (10)–(13) where D_e is the diffusion coefficient in the solid, $N_{e,k}$ denotes the flux of lithium ions in the electrolyte within the region k, and $x \in [0, L]$ is the macroscopic through-cell distance. This equation is also solved subject to continuity of concentration and flux at the electrode/separator interfaces.

$$\in_k \frac{\partial_{c_{e,k}}}{\partial_{\mathrm{t}}} = -\frac{\partial N_{e,k}}{\partial \mathrm{x}} + \begin{cases} \dfrac{1}{FL_n}, & k=n \\ 0, & k=s \\ \dfrac{1}{FL_p}, & k=p \end{cases} \tag{10}$$

$$\mathrm{N_{e,k}} = -\in_k^{\,b} D_e \frac{\partial_{c_{e,k}}}{\partial \mathrm{x}} + \begin{cases} \dfrac{xt+IRT}{FL_n}, & k=n \\ \dfrac{t+IRT}{F}, & k=s \\ \dfrac{(1-x)t+IRT}{FL_p}, & k=p \end{cases} \tag{11}$$

$$\mathrm{N_{e,n}}\,|_{x=0} = 0, \mathrm{N_{e,p}}\,|_{x=L} = 0 \tag{12}$$

$$\frac{\partial_{c_{s,k}}}{\partial_{\mathrm{t}}} = -\frac{1}{r_k^2}\frac{\partial}{\partial_{r_k}}\left(r_k^2 \mathrm{N_{s,k}}\right) \tag{13}$$

Voltage formulas are given in (14)–(22) where U_k is the reference OCP, b is the Bruggeman coefficient, j is the exchange-current density, ϕ is the electric potential, F is the Faraday's constant, R is the universal gas constant, and T is the temperature, L_n,L_s,L_p are the thicknesses of the negative electrode, separator, and positive electrode respectively.

$$V = U_{eq} + \eta_r + \eta_c + \Delta\Phi_{Elec} + \Delta\Phi_{Solid} \tag{14}$$

$$U_{eq} = U_p(c_p)\,|_{r_p=1} - U_n(c_n)\,|_{r_n=1}, \tag{15}$$

$$\eta_r = -2\sinh^{-1}\left(\frac{I}{\bar{j}_{0,p}L_p}\right) - 2\sinh^{-1}\left(\frac{I}{\bar{j}_{0,n}L_n}\right) \tag{16}$$

$$\eta_c = 2\left(1-t^+\right)\frac{RT}{F}\left(\bar{c}_{e,p} - \bar{c}_{e,n}\right) \tag{17}$$

$$\bar{j}_{0,n} = \frac{1}{L_n}\int_0^{L_n} \frac{\gamma_n}{C_{r,n}}\left(c_n\right)^{1/2}\left(1-c_n\right)^{1/2}\left(1+C_e c_{e,n}\right)^{1/2} dx \tag{18}$$

$$\bar{j}_{0,p} = \frac{1}{L_p}\int_{1-L_p}^{L_p} \frac{\gamma_p}{C_{r,p}}\left(c_p\right)^{1/2}\left(1-c_p\right)^{1/2}\left(1+\;\; C_e c_{e,p}\right)^{1/2} dx \tag{19}$$

$$\Delta\phi_{Elec} = -\frac{C_e I}{\gamma_e \kappa_e(1)}\left(\frac{L_n}{3\,{}_n^{\,b}} + \frac{L_s}{{}_s^{\,b}} + \frac{L_n}{3\,{}_p^{\,b}}\right) \tag{20}$$

$$\Delta\Phi_{Solid} = -\frac{I}{3}\left(\frac{Lp}{\sigma_p} + \frac{L_n}{\sigma_n}\right) \tag{21}$$

$$\bar{c}_{e,n} = \frac{1}{L_n}\int_0^{L_n} c_{e,n}dx, \; \bar{c}_{e,p} = \frac{1}{L_p}\int_{L-L_p}^{L_n} c_{e,p}dx \tag{22}$$

C. Doyle–Fuller–Newman Model

The Doyle–Fuller–Newman (DFN) model introduced and developed by Doyle and Newman is a widely used electrochemical model for simulating the operation of lithium-ion batteries [Fig. 3]. It integrates mass transfer, diffusion, migration, and reaction kinetics to provide a comprehensive understanding of battery behavior.

The DFN model is acknowledged as the most widespread and extensively verified model in the literature for investigating Li-ion batteries. It is made up of equations describing the movement of lithium ions within the battery electrodes and electrolyte. These equations are essentially based on partial differential equations (PDEs) governing diffusion phenomena.

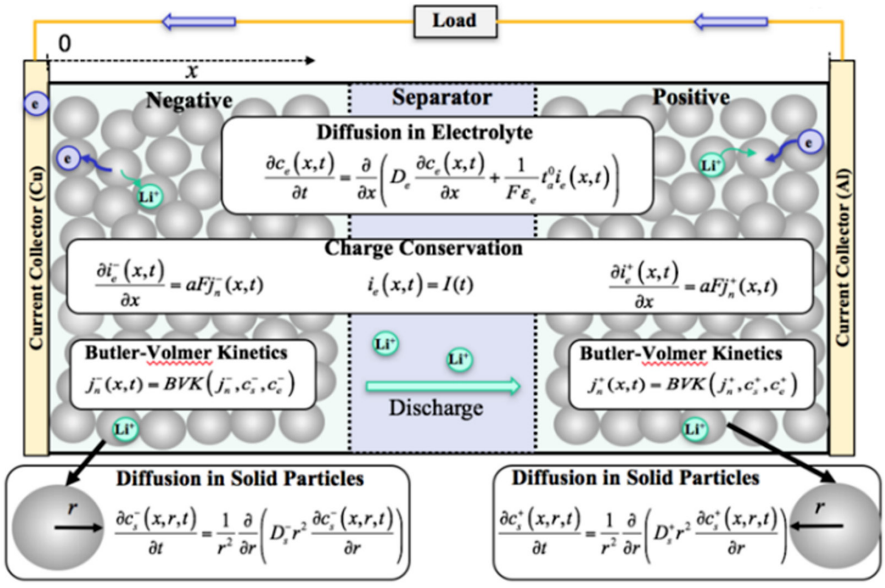

Fig. 3. DFN model of lithium-ion batteries [32]. DFN, Doyle–Fuller–Newman.

In particular, diffusion PDEs in solid particles are very crucial in the DFN model. They provide significant information about the presence of lithium ions for electrochemical reactions and the lithium concentration within the electrodes. However, resolving these solid-phase diffusion equations needs more computational work compared to the electrolyte phase diffusion equations. This is mainly because solid-phase diffusion changes not only through the thickness of the electrode on the macroscopic scale (x-scale), but also through the radius of the particles on the microscopic scale (r-scale).

The DFN model is composed of coupled PDAEs, and some of the parameters in these equations are coupled together such that it is mathematically not possible to determine all parameter values correctly and uniquely from input–output data [27]. Exact parameterization is difficult as many of the required quantities must be inferred indirectly from experimental data. Moreover, there can be significant variability from device to device, even in cells that are seemingly prepared in the same way. Therefore, proper parameterization is an obstacle that must be addressed to obtain the maximum benefit from DFN models [28]. Due to the computational complexity of solid phase diffusion, efforts are being made to simplify these equations to allow for real-time simulation capabilities. This simplification is very important for practical applications where rapid prediction of battery performance is necessary [31].

Overall, the DFN model is a strong tool for investigating the electrochemical behavior of Li-ion batteries and offers insights into the various processes that occur within the battery during charge-discharge cycles.

More detailed explanation of DFN and its formulas, DFN model encapsulates equations ensuring the conservation of charge and mass within both the solid and electrolyte phases, while also outlining the behavior governing electrochemical reactions transpiring at the interface between the solid and electrolyte [32, 33]. A Roman subscript is employed to signify the negative electrode, separator, and positive electrode regions, respectively. The model equations for the DFN are as follows [24, 30, 34]:

Charge conservation formulas are given in (23)-(25) where a_k is the electrode surface area density, ^{k} is the electrolyte volume fraction, c_e is the lithium-ion concentration in the electrolyte, a_k is the electrode surface area density, i is the current density:

$$\frac{\partial i_{e,k}}{\partial x} = \begin{cases} a_k j_k, k = n,p \\ 0, \quad k = s \end{cases} \tag{23}$$

$$i_{e,k} = {}^{b}_{k}K_e\left(c_{e,k}\right)\left(-\frac{\partial \phi_{e,k}}{\partial x} + 2\left(1-t^{+}\right)\frac{RT}{F}\frac{\partial}{\partial x}\left(\log(c_{e,k})\right)\right), k \in n,s,p \tag{24}$$

$$I - i_{e,k} = -\sigma_k \frac{\partial \phi_{e,k}}{\partial x}, \quad k \in p\ s,p \tag{25}$$

Mass conservation formulas are given in (26)-(29) where N is the molar flux and D_e is the electrode diffusivity:

$${}_{k}\frac{\partial c_{e,k}}{\partial t} = -\frac{\partial N_{e,k}}{\partial x} + \frac{1}{F}\frac{\partial i_{e,k}}{\partial x}, k \in n,s,p \tag{26}$$

$$N_{e,k} = {}^{b}_{k}D_e\left(c_{e,k}\right)\frac{\partial c_{e,k}}{\partial x} + \frac{t^{+}}{F}i_{e,k}, \quad k \in n,s,p \tag{27}$$

$$\frac{\partial c_{s,k}}{\partial t} = -\frac{1}{r_k^2}\frac{\partial}{\partial_{r_k}}\left(r_k^2 N_{s,k}\right), \quad k \in n,p \tag{28}$$

$$N_{s,k} = -D_{s,k}\left(c_{s,k}\right)\frac{\partial_{c_{s,k}}}{\partial_{r_k}}, \quad k \in n,p. \tag{29}$$

Electrochemical reaction formulas are given in (30)-(32):

$$j_k = 2j_{0,k}\sinh\left(\frac{F\eta_k}{2RT}\right), k \in n,p, \tag{30}$$

$$j_{0,k} = c_{s,k}^{\frac{1}{2}}\left(1-c_{s,k}\right)^{\frac{1}{2}} c_{e,k}^{\frac{1}{2}}\big|_{r_k=1}, k \in n,p \tag{31}$$

$$\eta_k = \phi_{s,k} - \phi_{e,k} - U_k\left(c_{s,k}\big|_{r_k=1}\right), \quad k \in n,p, \tag{32}$$

Current formulas are given in (33)–(35):

$$i_{e,n}\big|_{x=0} = 0, \quad i_{e,p}\big|_{x=L} = 0, \tag{33}$$

$$\phi_{e,n}\big|_{x=L_n} = \phi_{e,s}\big|_{x=L_n},\ i_{e,n}\big|_{x=L_n} = i_{e,s}\big|_{x=L_n} = I \tag{34}$$

$$\phi_{e,s}\big|_{x=L-L_p} = \phi_{e,p}\big|_{x=L-L_p}, \quad i_{e,s}\big|_{x=L-L_p} = i_{e,p}\big|_{x=L-L_p} = I \tag{35}$$

Concentration in the electrolyte is given in (36)-(38).

$$N_{e,n}\big|_{x=0} = 0, \quad N_{e,p}\big|_{x=L} = 0, \tag{36}$$

$$c_{e,n}\big|_{x=L_n} = c_{e,s}\big|_{x=L_n}, \quad N_{e,n}\big|_{x=L_n} = N_{e,s}\big|_{x=L_n}, \tag{37}$$

$$c_{e,s}\big|_{x=L-L_p} = c_{e,p}\big|_{x=L-L_p}, \quad N_{e,s}\big|_{x=L-L_p} = N_{e,p}\big|_{x=L-L_p}. \tag{38}$$

Concentration in the electrode active material is given in (39):

$$N_{s,k}\big|_{r_k=0} = 0, \quad k \in n,p, \quad N_{s,k}\big|_{r_k=R_k} = \frac{j_k}{F}, \quad k \in n,p. \tag{39}$$

Reference potential is given in (40):

$$\phi_{s,cn} = 0, \quad x \in \partial\Omega_{\text{tab},n}. \tag{40}$$

Initial conditions are given in (41, 42):

$$c_{s,k}\left(x,r,0\right) = c_{s,k,0}, \quad k \in n,p \tag{41}$$

$$c_{e,k}\left(x,0\right) = c_{e,0}, \quad k \in n,s,p \tag{42}$$

III. COMPARISON OF ELECTROCHEMICAL BATTERY MODELS

By using the SPM, SPMe, and DFN model bases that have been described so far in this paper, all these models and cell types have been compared for different battery chemistries by using these different modeling techniques with the help of Python Pybamm Library [34] and Matlab platform has been used for the visualizations. Fig. 4 shows the results of the SPM, SPMe, and DFN models for a particular chemistry, LFP, using the Pybamm [30]. The model used in this comparison is the default model parameters available in Pybamm, and the mesh geometry and cell geometry are chosen by default. These default parameters were obtained from referenced papers [24, 30, 32-37]. Table I presents the computation times of the models.

In a comparative study on the solution times of the equations for DFN, SPM, and SPMe models, it has been observed that despite using the same solution methodology, the solution time for the DFN model is significantly longer compared to the SPM and SPMe models. This situation can be explained by the DFN model having a greater complexity in terms of the mathematical representation of the electrochemical processes considered within the model. This complexity directly affects the model's solution time, making it a significant factor in terms of time efficiency in analysis and simulation studies.

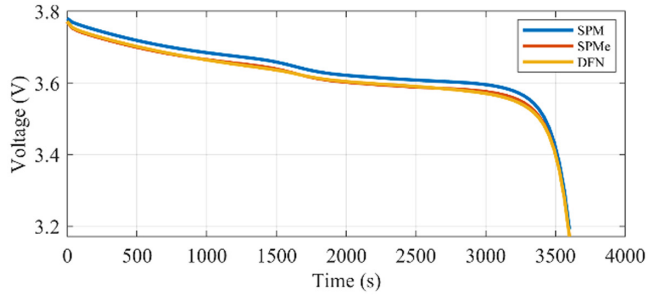

Fig. 4. Comparison of three different modeling types.

First, in Fig. 5, a comparison of 3 different modeling methods using lithium-ion polymer, Kokam SLPB 75106100, was performed at different C-rates and the total error values were compared. Parameters for a Kokam SLPB 75106100 cell are from the papers [19, 20]. The tab placement parameters are taken from measurements in [21]. The thermal material properties are for a power pouch cell by Kokam. The data are extracted from [34]. Lastly, the fits to data for the electrode and electrolyte properties are those provided by Dr. Simon O'Kane in the paper [6]. Also, the experimental data values were obtained from the 1C and 5C discharge values given in the cell datasheet.

Secondly, in Fig. 6, a comparison of three different modeling methods using Lithium cobalt oxide-graphite, Enertech LCOG SPB655060, was performed at different C-rates and the total error values were compared. Parameters for the Enertech cell, from the papers [22, 38] and references therein. SEI parameters are example parameters for SEI growth from the papers [38-43]. Also, the experimental data values were obtained from the 0.5C and 1C discharge values given in the cell datasheet.

Thirdly, in Fig. 7, a comparison of 3 different modeling methods using Lithium Iron Phosphate, A123 ANR26650M1B, was performed at different C-rates and the total error values were compared. Parameters for a Kokam SLPB 75106100 cell are from the papers [17]. Subsequently, a re-study was carried out and some of the parameters, in the article [18], were updated to give more accurate results. Nevertheless, it was noticed that even the values in the paper [18] did not exactly match the experimental data, so a

TABLE I.
COMPARISON OF THE COMPUTATION TIMES OF THE MODELS

Model	Computation time (ms)
Doyle–Fuller–Newman model	248.25
Single particle model with electrolyte	31.61
Single particle model	15.37

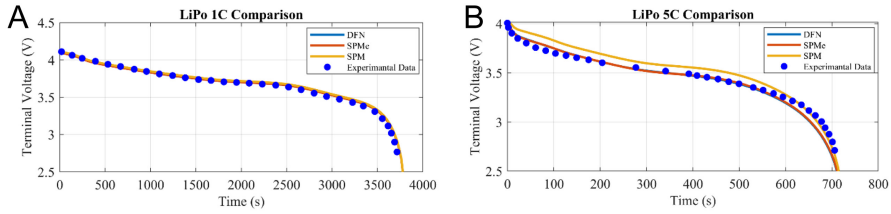

Fig. 5. Li-po modeling using DFN, SPMe, and SPM model with 1C and 5C C-rates. DFN, Doyle–Fuller–Newman; SPM, single particle model; SPMe, single particle model with electrolyte dynamics.

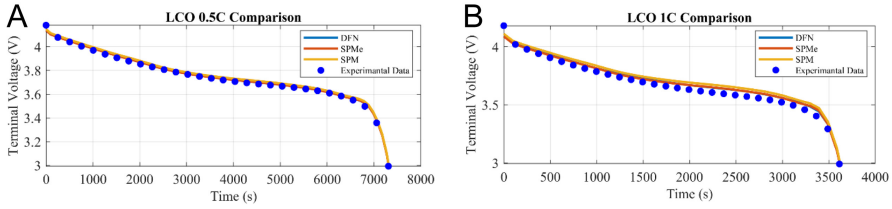

Fig. 6. LCO modeling using DFN, SPMe, and SPM model with 0.5C (a) and 1C (b) C-rates. DFN, Doyle–Fuller–Newman; SPM, single particle model; SPMe, single particle model with electrolyte dynamics.

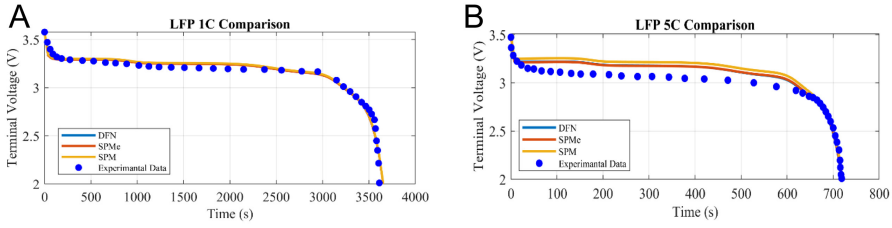

Fig. 7. LFP modeling using DFN, SPMe, and SPM model with 1C (a) and 5C (b) C-rates. DFN, Doyle–Fuller–Newman; SPM, single particle model; SPMe, single particle model with electrolyte dynamics.

parameter optimization technique was attempted. With this parameter optimization technique called curve fitting, curve fitting is the process of generating a curve or mathematical function that best fits a set of data points, possibly subject to restrictions, it was observed that more accurate values were achieved by adjusting the values of Negative electrode thickness and Negative particle radius as in Table II. The rest of the parameters remain the same as in [17].

Fourthly, in Fig. 8, the modeling of the INR21700 M50 battery cell, which is produced by LG Chem and features NMC 811 chemistry, was conducted. The analysis was carried out at a constant temperature of 25° Celsius, considering two different discharge current rates, 1C and 2C. The Pybamm Chen2020 parameters were utilized as the modeling parameters [44].

TABLE II.
OPTIMIZED VALUES

	Prada value [13]	Arksand value [14]	Optimized value
Negative electrode thickness [m]	3.6e−5	6.57e−5	3.46e−5
Negative particle radius [m]	5.86e−6	2.39e−05	7e−7

Drawing upon the acquired data, it becomes evident that the Discrete Fracture Network (DFN) model necessitates extensive mathematical computations and solution time in contrast to the Single Particle Model (SPM) and its extension, SPMe. For LiPo, LCO, LFP, and NMC battery cell types, results obtained using DFN, SMPe, and SPM models at various C-rate values have been compared with experimental data. Root mean square error calculations were performed for each model, and the results are presented in Table III.

As reported in Table IV, the comparison of all these models reveals that DFN has the highest overall score in terms of accuracy. It is followed by SPMe and SPM. Conversely, this order is exactly in reverse order in terms of complexity and computation time.

IV. CONCLUSION

This study provides a concise overview of physics-based modeling techniques found in existing literature and compares these

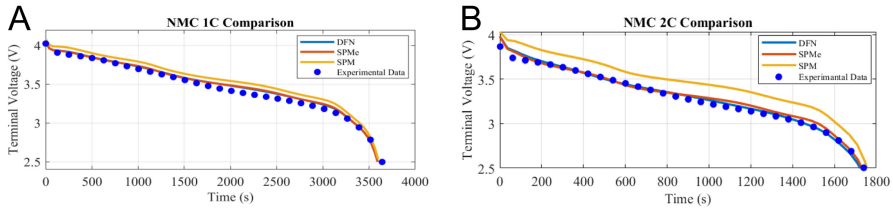

Fig. 8. NMC modeling using DFN, SPMe, and SPM model with 1C (a) and 2C (b) C-rates. DFN, Doyle–Fuller–Newman; SPM, single particle model; SPMe, single particle model with electrolyte dynamics.

TABLE III.
RMS ERRORS (MV) FOR VARIOUS BATTERY TYPES AND C-RATES

Battery Types	**LiPo**		**LCO**		**LFP**		**NMC**	
Model/Crates	**1C**	**5C**	**0.5C**	**1C**	**1C**	**5C**	**1C**	**2C**
DFN	38.6	66.2	13.3	36.6	65.7	78.2	44.8	34
SPMe	38.8	67	22.8	36.9	66	79	47.5	42.9
SPM	47.6	78.2	25.2	66	66.4	100.9	97	175.3

TABLE IV.
COMPARISON OF EACH BATTERY MODEL

Model	**DFN**	**SPMe**	**SPM**
Accuracy	+++	++	+
Complexity	+	++	+++
Computation time	+	++	+++

DFN, Doyle–Fuller–Newman; SPM, single particle model; SPMe, single particle model with electrolyte dynamics.

methodologies in terms of their complexity and predictive capabilities. Furthermore, it explores the relationship between these modeling approaches and specific chemical compositions. During the investigation, several modeling techniques from the literature were refined using optimization methods to enhance accuracy. By scrutinizing the modeling outcomes in detail, efforts were made to identify which chemical compositions align more accurately with particular modeling methodologies, as well as identifying chemistries that are more amenable to physics-based modeling. Future research endeavors may prioritize standardizing parameterization procedures and discharge-charge tests within laboratory settings to enhance data precision, while also incorporating machine learning techniques to improve the accuracy of battery parameters. The integration of machine learning and physics-based modeling holds promise for the development of advanced models, facilitating a deeper comprehension of battery dynamics and contributing to the continuous advancement of battery technology.

Peer-review: Externally peer-reviewed.

Author Contributions: Concept – H.Y., A.A.; Design – H.Y., A.A.; Supervision – M.O.G.; Resources – M.O.G.; Materials – H.Y., A.A.; Data Collection and/or Processing – H.Y., A.A.; Analysis and/or Interpretation – H.Y., A.A., M.O.G.; Literature Search – H.Y., A.A., M.O.G.; Writing – H.Y., A.A., M.O.G.; Critical Review – M.O.G.

Declaration of Interests: The authors have no conflicts of interest to declare.

Funding: This work was supported by İstanbul Technical University (ITU) Scientific Research Projects Unit (BAP) under Project MGA-2022-43948 and in part by the 1004 - Center of Excellence Support Program of TUBITAK under Project 22AG018.

REFERENCES

1. J. Meng, G. Luo, M. Ricco, M. Swierczynski, D. I. Stroe, and R. Teodorescu, "Overview of lithium-Ion battery modeling methods for state-of-charge estimation in electrical vehicles," In *Appl. Sci. (Switzerland)*, vol. 8, no. 5, 2018. [CrossRef]
2. R. Dima, G. Buonanno, S. Costanzo, and R. Solimene, "Robustness for the starting point of two iterative methods for fitting debye or cole–cole models to a dielectric permittivity spectrum," *Appl. Sci. (Switzerland)*, vol. 12, no. 11, 2022. [CrossRef]
3. J. Manwell, and J. McGowan, "Extension of the kinetic battery model for wind/hybrid power systems". 5th European Wind Energy Association Conference and Exhibition (EWEC '94), 1994.
4. L. E. Unnewehr, and S. A. Naser, "Electric vehicle technology,",". 1982. Available: https://www.osti.gov/biblio/5030604.
5. H. Arunachalam, S. Onori, and I. Battiato, "On veracity of macroscopic lithium-ion battery models," *J. Electrochem. Soc.*, vol. 162, no. 10, A1940–A1951, 2015. [CrossRef]
6. C. Capasso, and O. Veneri, "Experimental analysis on the performance of lithium based batteries for road full electric and hybrid vehicles," *Appl. Energy*, vol. 136, 921–930, 2014. [CrossRef]
7. X. Hu, F. Sun, Y. Zou, and H. Peng, "Online estimation of an electric vehicle lithium-Ion battery using recursive least squares with forgetting,", in *Proceedings of the American Control Conference*, 2011, 935–940. [CrossRef]
8. A. A. H. Hussein, and I. Batarseh, "An overview of generic battery models," *IEEE Power Energy Soc. Gen. Meet.*, 1–6, 2011. [CrossRef]

9. B. Steven, C. H. Applied, and S. C. Hageman, *Using PSpice to Simulate the Discharge Behavior of Common Batteries. EDN Magazine*, 1993.
10. O. Karahan, A. Özan, and M. Bağriyanik, "The effects of mobile battery energy storage systems on the distribution network," *Turk J. Electr. Power Energy Syst.*, vol. 1, no. 2, pp. 69–74, 2021. [CrossRef]
11. G. Alexander, and H. Anton, "Parametrization of A simplified physical battery model," *Proceedings of the 13th International Modelica Conference*, Regensburg, Germany, vol. 157, 215–220, 2019. [CrossRef]
12. W. Li *et al.*, "Parameter sensitivity analysis of electrochemical model-based battery management systems for lithium-ion batteries," *Appl. Energy*, vol. 269, 2020. [CrossRef]
13. P. Domingos, "A few useful things to know about machine learning," In *Commun. ACM*, vol. 55, no. 10, 78–87, 2012. [CrossRef]
14. V. Lucaferri, M. Quercio, A. Laudani, and F. Riganti Fulginei, "A review on battery model-based and data-driven methods for battery management systems," *Energies*, vol. 16, no. 23, p. 7807, 2023. [CrossRef]
15. N. Watrin, H. Ostermann, B. Blunier, and A. Miraoui, "Multiphysical lithium-based battery model for use in state-of-charge determination," *IEEE Trans. Veh. Technol.*, vol. 61, no. 8, 3420–3429, 2012. [CrossRef]
16. J. C. Forman, S. Bashash, J. L. Stein, and H. K. Fathy, "Reduction of an electrochemistry-based Li-ion battery model via quasi-linearization and Padé approximation," *J. Electrochem. Soc.*, vol. 158, no. 2, 2011. [CrossRef]
17. E. Prada, D. di Domenico, Y. Creff, J. Bernard, V. Sauvant-Moynot, and F. Huet, "A simplified electrochemical and thermal aging model of LiFePO 4 -Graphite Li-ion batteries: Power and capacity fade simulations," *J. Electrochem. Soc.*, vol. 160, no. 4, A616–A628, 2013. [CrossRef]
18. "Parametrization of a lithium- ion battery Elsa Arksand Kth Royal Institute of Technology School of Engineering Sciences in Chemistry, Biotechnology and Health." Available: https://www.diva-portal.org/smash/get/diva2:1593557/FULLTEXT02. [Accessed: Mar. 27, 2024].
19. M. Ecker, S. Käbitz, I. Laresgoiti, and D. U. Sauer, "Parameterization of a physico-chemical model of a lithium-ion battery," *J. Electrochem. Soc.*, vol. 162, no. 9, A1849–A1857, 2015. [CrossRef]
20. M. Guo, G. Sikha, and R. E. White, "Single-particle model for a lithium-ion cell: Thermal behavior," *J. Electrochem. Soc.*, vol. 158, no. 2, 2011. [CrossRef]
21. A. Hales, L. B. Diaz, M. W. Marzook, Y. Zhao, Y. Patel, and G. Offer, "The cell cooling coefficient: A standard to define heat rejection from lithium-ion batteries," *J. Electrochem. Soc.*, vol. 166, no. 12, A2383–A2395, 2019. [CrossRef]
22. W. Ai, L. Kraft, J. Sturm, A. Jossen, and B. Wu, "Electrochemical thermal-mechanical modelling of stress inhomogeneity in lithium-ion pouch cells," *J. Electrochem. Soc.*, vol. 167, no. 1, 2020. [CrossRef]
23. F. Brosa Planella *et al.*, "A continuum of physics-based lithium-ion battery models reviewed," *Prog. Energy*, vol. 4, no. 4, 2022. [CrossRef]
24. J. A. E. Andersson, J. Gillis, G. Horn, J. B. Rawlings, and M. Diehl, "CasADi: A software framework for nonlinear optimization and optimal control," *Math. Program. Comput.*, vol. 11, no. 1, 1–36, 2019. [CrossRef]
25. M. Ahmadi, "Presentation of the new method for simultaneous estimation of the parameters and the charge situation of used batteries in hybrid vehicles," *Turk J. Electr. Power Energy Syst.*, vol. 2, no. 2, pp. 103–114, 2022. [CrossRef]
26. L. V. Raviteja, and G. Gurrala, "A review of lithium-ion battery physics-based models," In *IEEE Power Energy Soc. Gen. Meet. (PESGM)*, vol. 2023, (pp. 1–5). Orlando, USA., 2023. [CrossRef]
27. E. Miguel, G. L. Plett, M. S. Trimboli, L. Oca, U. Iraola, and E. Bekaert, "Review of computational parameter estimation methods for electrochemical models," *J. Energy Storage*, vol. 44, no. B, p. 103388. ISSN 2352-152X, 2021. [CrossRef]
28. A. A. Wang *et al.*, "Review of parameterisation and a novel database (LiionDB) for continuum Li-ion battery models," *Prog. Energy*, vol. 4, no. 3, p. 032004, 2022. [CrossRef]
29. J. Zhou, B. Xing, and C. Wang, "A review of lithium-ion batteries electrochemical models for electric vehicles," In, *E3S Web Conf.* EDP Sciences, vol. 185, 2020. [CrossRef]
30. S. G. Marquis, V. Sulzer, R. Timms, C. P. Please, and S. J. Chapman, "An asymptotic derivation of a single particle model with electrolyte," *J. Electrochem. Soc.*, vol. 166, no. 15, A3693–A3706, 2019. [CrossRef]
31. N. Jin, D. L. Danilov, P. M. J. van den Hof, and M. C. F. Donkers, "Parameter estimation of an electrochemistry-based lithium-ion battery model using a two-step procedure and a parameter sensitivity analysis," *Int. J. Energy Res.*, vol. 42, no. 7, 2417–2430, 2018. [CrossRef]
32. W. He, M. Pecht, D. Flynn, and F. Dinmohammadi, "A physics-based electrochemical model for lithium-ion battery state-of-charge estimation solved by an optimised projection-based method and moving-window filtering," *Energies*, vol. 11, no. 8, 2018. [CrossRef]
33. J. C. Forman, S. J. Moura, J. L. Stein, and H. K. Fathy, "Genetic identification and fisher identifiability analysis of the Doyle-Fuller-Newman model from experimental cycling of a LiFePO 4 cell," *J. Power Sources*, vol. 210, 263–275, 2012. [CrossRef]
34. V. Sulzer, S. G. Marquis, R. Timms, M. Robinson, and S. J. Chapman, "Python battery mathematical modelling (PyBaMM)," *J. Open Res. Softw.*, vol. 9, no. 1, 2021. [CrossRef]
35. T. Tranter *et al.*, "liionpack: A Python package for simulating packs of batteries with PyBaMM," *J. Open Source Softw.*, vol. 7, no. 70, 2022. [CrossRef]
36. M. Doyle, T. F. Fuller, and J. Newman, "Modeling of galvanostatic charge and discharge of the lithium/polymer/insertion cell," *J. Electrochem. Soc.*, vol. 140, no. 6, 1526–1533, 1993. [CrossRef]
37. R. Deshpande, M. Verbrugge, Y.-T. Cheng, J. Wang, and P. Liu, "Battery cycle life prediction with coupled chemical degradation and fatigue mechanics," *J. Electrochem. Soc.*, vol. 159, no. 10, A1730–A1738, 2012. [CrossRef]
38. B. Rieger, S. V. v. Erhard, K. Rumpf, and A. Jossen, "A new method to model the thickness change of a commercial pouch cell during discharge," *J. Electrochem. Soc.*, vol. 163, no. 8, A1566–A1575, 2016. [CrossRef]
39. P. Ramadass, B. Haran, P. M. Gomadam, R. White, and B. N. Popov, "Development of first principles capacity fade model for Li-ion cells," *J. Electrochem. Soc.*, vol. 151, no. 2, 2004. [CrossRef]
40. H. J. Ploehn, P. Ramadass, and R. E. White, "Solvent diffusion model for aging of lithium-ion battery cells," *J. Electrochem. Soc.*, vol. 151, no. 3, 2004. [CrossRef]
41. F. Single, A. Latz, and B. Horstmann, "Identifying the mechanism of continued growth of the solid–electrolyte interphase," *ChemSusChem*, vol. 11, no. 12, 1950–1955, 2018. [CrossRef]
42. M. Safari, M. Morcrette, A. Teyssot, and C. Delacourt, "Multimodal physics-based aging model for life prediction of Li-ion batteries," *J. Electrochem. Soc.*, vol. 156, no. 3, 2009. [CrossRef]
43. X. G. Yang, Y. Leng, G. Zhang, S. Ge, and C. Y. Wang, "Modeling of lithium plating induced aging of lithium-ion batteries: Transition from linear to nonlinear aging," *J. Power Sources*, vol. 360, 28–40, 2017. [CrossRef]
44. C.-H. Chen, F. Brosa Planella, K. O'Regan, D. Gastol, W. D. Widanage, and E. Kendrick, "Development of experimental techniques for parameterization of multi-scale lithium-ion battery models," *J. Electrochem. Soc.*, vol. 167, no. 8, 2020. [CrossRef]